

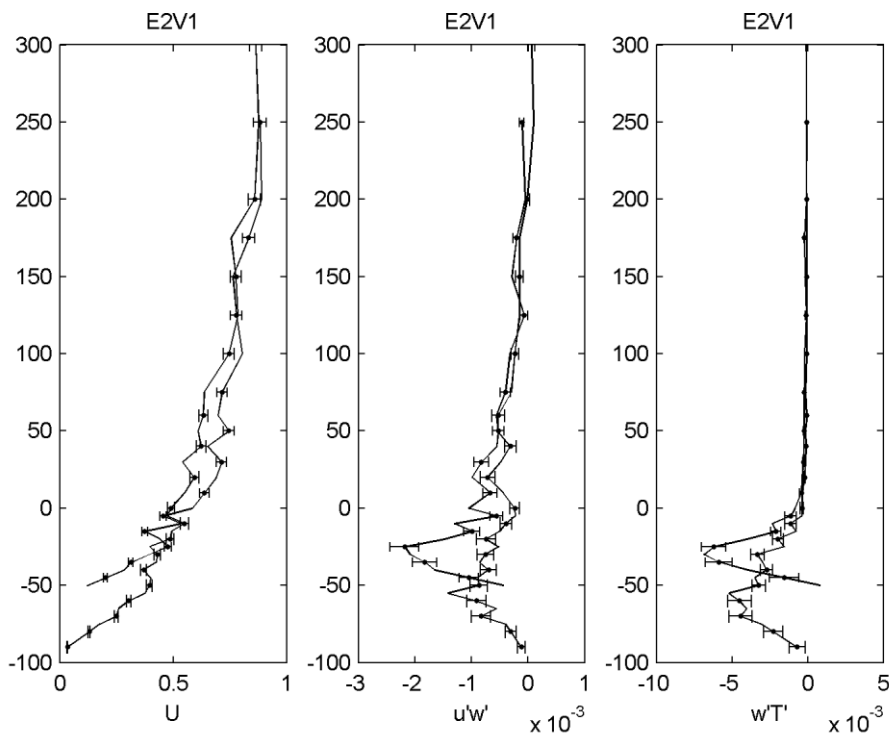
*Response to Reviewer 1:*

We thank Reviewer 1 for her/his valuable comments on the manuscript. We answered below to all his/her points.

**Major remarks:**

**1. Uncertainty estimates:** The graphs present the results for the mean flow and the turbulent fluxes. However, these values will have a certain uncertainty that is not discussed in the paper. These uncertainties contain instrument uncertainties, uncertainties in the representation, as well as due to statistical uncertainties (since I assume that the presented profiles are the result of averaging many repeating results). My experience with analogous experiments is that these uncertainties can be substantial, and they need to be quantified.

Response: Following your advice we estimated the uncertainty of mean quantities and turbulent fluxes. We now show profiles of uncertainty for each measurement point calculated from the formula below. Due to readability of profiles, we decided to show the figures in the supplement of the manuscript. We present here one example figure (Figure 1) showing the profiles of wind velocity and turbulent momentum and heat flux of experiment E2V1 with its uncertainty estimates as error bar for each point.



We added the following paragraph to the method section:

*We estimated the uncertainty, considering both the systematic and random components.*

*The random uncertainty is significantly larger than the systematic uncertainty. The random*

*uncertainty was considered as follows:  $u_q = \frac{\sigma_q}{\langle q \rangle \sqrt{N}}$*

*with  $N$  the number of independent samples separated by the integral-time scale of  $u$ . We did not appreciate significant differences applying the method of \citet{Mann}, therefore we adopted the simplest method. We spatially averaged the total uncertainty (systematic and random) within the first 0.1 m from the snow surface where turbulent mixing is mainly occurring. The uncertainties of the mean streamwise velocity and temperature fall below 3.3%. The uncertainties of the fluxes are larger and between 9% and 33%. The large uncertainties of the fluxes reflect the high level of turbulence in the flow together with the mean values approaching to zero towards the surface.*

**2. A key advantage of a wind tunnel is the fact that experiments can be reproduced by repeating the experiment under similar conditions. How many times have the reported experiments been repeated? Repeating the experiments will strengthen the statistical robustness of the results.**

Response: In general, it is true that the wind tunnel has the advantage to repeat measurements several times under similar conditions. You should, however, keep in mind that we measured flow fields above a melting snow cover under typical spring conditions. This means, that we could only perform measurements in spring or autumn. We conducted our experiments on a manually designed concave depression made with compacted natural snow. The procedure we adopted allowed the construction with sufficient precision. Much care was taken to ensure smooth transition between the upstream fetch and the snow-fetch as well as to construct a smooth concave section. Even if we could have rebuilt the snow concave section for further tests we might not have been able to achieve the accuracy required to replicate exactly the same surface in the test section, thus we could not repeat our experiments without affecting the flow and significantly increasing the measurement uncertainty. In summary, repeating the measurements had the following limitations:

- Measurements could be only performed during typical spring conditions: when natural snow has been available and temperatures are clearly above the melting point but also not too high to create untypically stable conditions
- All measurements had to be finished within one day and within a few hours of that day, when air temperatures were high enough during daytime
- The snow cover was melting and we had to prepare the snow cover for each single experimental design. Although the snow cover was prepared carefully, small differences in the surface characteristics between single measurement days were present that added an additional degree of uncertainty to the measurements (see uncertainty)

**3. Eddy correlation technique: I do agree with applying the “eddy correlation technique” in the study, and its application over a flat surface is correct. However, for the sloping terrain in the E2 experiments the so called planar fit corrections (as described in Wilczak et al 2001) should be applied. Has that been done?**

Response: In the original version we decided to keep the same coordinate system for both measurement locations. We now applied the planar fit approach for X1 to correct the data following Wilczak et al 2001 and changed the figures accordingly. The results show, however, only minor changes to the prior one and do not change the typical shape of the flux profiles.

**4. Scaling: All results have been presented after scaling. The applied scaling (with the flow speed above the boundary layer and the temperature difference between ambient and surface temperature) closely follows the routine in the engineering community. I was wondering whether the authors tried to apply the traditional Monin-Obukhov similarity, in which local fluxes scale with the local gradients of temperature and wind speed. The experimental results to provide sufficient information to do so, isn't it? By applying the results will connect more to the knowledge in the field of boundary-layer meteorology.**

Response: We thank the reviewer for this suggestion. We feel, however, that considering the scope of the study, profiles of local fluxes scaled with the related local gradient will not add a substantial value to the conclusions of the study. While it is correct that local scaling is applied in particular for stable conditions (Nieuwstadt et al. 1984, 1985), we are interested in the bulk effect when stratification interacts with local topography. Since the main goal is the investigation of boundary layer decoupling above a melting snow cover under typical spring conditions (small temperature gradients) and over different surface shapes, we are interested in the direct measurement of turbulence profiles. Instead of scaling local fluxes with the related gradient we introduced profiles of the Richardson number to show the ratio between buoyancy produced turbulence to turbulence generated by shear (see figure 8a). This has the advantage for the community to interpret the results with respect to typical "law of the wall" parameterizations used in numerical models.

Nieuwstadt, F. T. M.: Some aspects of the turbulent stable boundary layer, *Bound.-Lay. Meteorol.*, 30, 31–55, 1984.

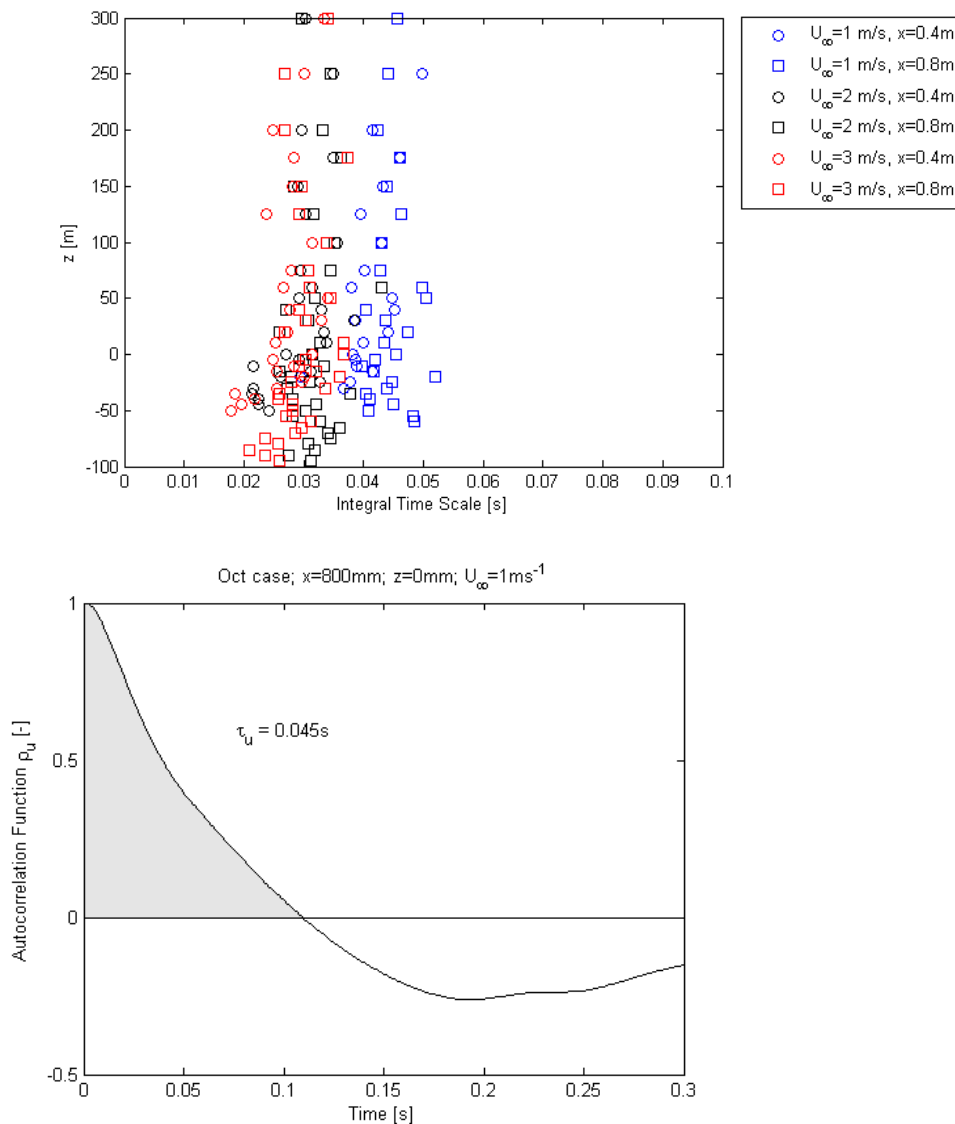
Nieuwstadt, F. T. M.: A model for the stationary, stable boundary layer, in: *Turbulence and Diffusion in Stable Environments*, edited by: Hunt, J. C. R., Clarendon Press, 149-179, 1985.

**5. More scaling: For a the applied scaling (i.e. without time as a scaling variable), it is important that stationarity is reached during the experiment. This is unfortunately not discussed in the paper.**

Response:

We applied high-pass filtering to the acquired time-series to avoid potential contamination from low-frequency waves from the approaching flow. For the experimental design we had to ensure statistical representativeness of the results. Therefore we conducted experiments with a long acquisition (100s) for the flat case, where the experimental design allowed that, to ensure high statistical stationarity of the fluxes. Unfortunately the need to complete our experiments in a given time before the melting process would cause appreciable changes in the snow surface shape, led us to reduce the duration of the acquisition in case of the concave section. We designed our experiments by sampling the flow at least hundred times the integral time scale (Tropea, C., Yarin, A.L. and Foss, J.F. eds., 2007. Springer handbook of experimental fluid mechanics. Springer Science & Business Media). As shown in the figure below (Fig. 1) the integral time scale ranges between 0.02 and 0.05 for all the experiments. The choice to sample for 20 s in case of the concave section represented a reasonable compromise between the need of the two requirements. Fig. 2 shows an

example of the resulting integral time scale obtained by integrating the area below the autocorrelation function until this reaches zero.



We will include a short note on stationarity of the flow to the methods section and also add the figures to the supplement.

**6. Definition of low-level jet and drainage flows. Multiple times the terms low-level jet, drainage flows, and wind maxima are used, but a formal definition is missing. I can imagine that the winds in experiment E2 will accelerate just after the pool has been reached, since the horizontal flow suddenly does not feel a underlying surface anymore. This has however not much to do with stratification or winds in the pool. However, can one call this a low-level jet then? Baas et al (2008) and Tuononen et al (2015) can provide some guidance on how to define low-level jets and other wind maxima in a more objective way.**

Response: we thank the reviewer for this comment. We agree that the wind velocity maxima are not strong enough (also compared to the well-defined criteria of Tuonen et al., 2015) to call it a pronounced LLJ. We changed this throughout the paper and also do not link that

peak to a drainage flow anymore. We agree with the reviewer that the flow acceleration is primarily due to the detachment of the flow from the surface. We changed the text accordingly: *The low-level maxima in velocity might be caused by the acceleration of the flow behind the topographical step (the highest point of the cavity) due to the detachment from the surface.*

**7. In the introduction the authors mention that numerical models do often not account for cold air pooling. However, the paper does not pick up the opportunity to indicate the implications for modelling studies. I.e. how should model developers modify flux parameterizations in classic surface-layer parameterizations to account for the pooling effects?**

Response: In the introduction part we mention that numerical models fail to reproduce boundary layer decoupling at the lowest few centimetres above the ground mainly due to the vertical resolution. We do not have an explicit advice for modellers how to easily modify classic surface-layer parametrizations to account for boundary layer decoupling. This is beyond the scope of this study. Measurements show that low wind velocities and sheltering promotes boundary layer decoupling over melting snow surfaces. Applying LES models a sufficiently high vertical resolutions close to the ground will allow simulating this effect. We now explicitly refer to LES models in the intro-part: *Applying Large-eddy simulations, high horizontal resolution of at least 5 m are necessary to adequately represent the formation of thermal internal boundary layers. What cannot be captured with that resolutions is the strong suppression of turbulence due to strong atmospheric stability at the lowest centimetres above the snow surface* \citep{mott15}.

**8. Structure: In my opinion the conclusion section is too long and mixed with a discussion at the same time. Please consider to set up clearly delineated “discussion” and “conclusion” sections, each with their unique role**

Response: The conclusion and discussion sections are revised accordingly. All parts discussing the results are moved to the newly introduced section: *Discussion: Indications of boundary layer decoupling within the cavity.*

**Minor remarks:**

**P5414, In 4: ...from the atmosphere to the snow surface. Just to make clear that you do not hint to the heat flux from the underlying snow/ice.**

Response: changed

**P5414, In 16-18: Remove “Further work....temperatures”**

Response: we agree with the reviewer and skip the last sentence of the abstract.

**P5415, In 15: “Bruns” should be “Burns”**

Response: changed

**P5415, In 20: “Bruns” should be “Burns”**

Response: changed

**P5415, In 23: “A special case”: please be more precise what you mean with special case. Is it special because cold-air pooling is poorly understood, or because cold-air pooling does infrequently occur?**

Response: We agree with the reviewer that this statement is not very precise. We changed the sentence to: *Cold-air pooling can also occur over snow fields that are located within topographical depressions where associated atmospheric decoupling is mainly driven by the cooling effect of the underlying snow on the air.*

**P5416, In 9-13: I slightly disagree with this statement, since in very stable cases the boundary layer becomes rather shallow, and therefore measurements with a relatively short tower can characterize the complete stable boundary layer.**

Response: Yes, but only if a high number of sensors is used to measure the vertical profile and only if sensors with very small path lengths are used to measure small eddies close to the surface. We added these specifications to the manuscript:

*In the field, atmospheric profiles obtained from eddy-correlation measurements are typically based on a few measurement points, which makes it difficult to capture boundary layer dynamics of shallow internal thermal boundary layers. Especially turbulent heat fluxes close to the snow surface are difficult to measure in the field because of the relatively large path lengths of sonic anemometers and consequentially the low vertical resolution of measurement points close to the surface. Although measurements conducted by Mott et al. (2013) indicated that boundary layer decoupling over a melting snow patch especially occurred during low ambient wind velocities, the effect of the topography via sheltering could not be analysed because the “varying one parameter at a time” approach is difficult if not impossible to achieve in the field.*

**P5416, In 9-13: Please also discuss the role of the footprint under the various ranges of wind speed.**

Response: We now discuss the role of footprint in the discussion part:

*Comparing the flux profiles of the different experiments and at different locations, we have to note that the locations measured at the downwind locations X1 and X2 will have varying footprints for the fluxes depending on wind speeds. At the same time, the differences between profiles at X1 and X2 give a first indication of how fluxes change in the streamwise direction. It is clear that lateral transport of heat and momentum plays an important role for the given conditions and that the net effect of a topographic depression on the boundary layer above still needs to be systematically analyzed.*

**P5416, In 19: “optimal”. Please rephrase this statement. Wind tunnel studies indeed do have their advantages over field observations, but they also have several disadvantages that should be acknowledged here. For example it is relatively difficult to obtain Reynolds numbers that are representative for the atmosphere. Are the Reynolds numbers in the current study comparable to atmospheric surface layer values ( $10^6$ )? Not according to Figure 8 (please comment). At the same time the authors do not mention the possibility of to repeat experiments as an advantage of wind tunnels studies.**

Response: Wind tunnel studies are not designed to match the full-scale Reynolds number. It is considered that as soon as the flow is turbulent (also in the near-surface layers) the flow is Reynolds number independent. In our case the presence of the upstream roughness elements increases the mechanical turbulence. We agree with the reviewer that field measurements also have clear advantages. We therefore changed the paragraph

accordingly: *Wind tunnels provide controlled conditions to measure the boundary layer dynamics above cooled surfaces* \citep{Ohya2001,Ohya2008}. Furthermore, the available measurement techniques also allow us to measure vertical profiles of turbulent quantities with a high vertical resolution of approximately 0.005 m (normalizing the vertical measurement resolution ( $\Delta z$ ) by boundary layer height ( $\delta$ ) in the wind tunnel ( $\Delta z/\delta$ ) this means 0.016). This comes at the expense of reduced eddy sizes and directional variation of winds in the tunnel.

**P5417, In 3-5:**The authors use melting snow here as medium to create stable conditions. However, I do not see the additional value of melting snow over melting ice, at least the impact of the snow roughness are not discussed in the paper. Could you please comment on this?

Response: Since we wanted to investigate the boundary layer above melting snow we did not see any advantage using ice instead, which of course has a different roughness length but is also more difficult to handle in the wind tunnel.

**P5417: Section 2.1:** the experimental setup is explained but the snow density, conductivity, etc is not discussed. Moreover I am curious whether temperature measurements were done in the snow pack? If the snowpack was vertically isotherm I do not expect heat conduction through the snow, but if this was not the case, heat conduction could play a role in the surface energy balance. The same holds for the melted snow that is penetrating the snow pack as liquid water. How has these processes been controlled?

Response: No temperature measurements were done in the snowpack, but the snowpack was already isotherm since the snowpack was already wet and melting. Thus, heat conduction did not play a role. We included the information of isothermal snowpack in the manuscript.

**P5418, In 3: “decoupling”:** multiple definitions for decoupling exist in the literature. It would strengthen the paper if a more formal definition of decoupling would be introduced, and be used to analyse the results.

Response: The reviewer is right that there are multiple definitions of decoupling in the literature. In this study we are especially interested in boundary layer decoupling that is characterized by a suppression of turbulence near the ground causing a significant reduction of vertical momentum transfer towards the ground (which would normally increase towards the surface where shear is strongest). We added this definition to the manuscript.

**P5420, In 15:** The Richardson number is mentioned here, but hardly used in the analysis later on, while it is an excellent quantity to characterize stratified flows as decoupling. For example, a vertical profile of Richardson number would provide more information than the vertical profile of the Reynolds number in Fig 8.

Response: we agree with the reviewer that a profile of the gradient Richardson number provides important insight into the ratio between buoyancy produced turbulence to turbulence generated by shear. Assuming a critical Richardson number of 0.25 (following Stull, 1988), results nicely show that the Richardson number only exceeds the critical value for the low wind velocity case and only within the concave section, further indicating

boundary layer decoupling for this case only. We added Figure 8a showing vertical profiles of the local Richardson number.

**P5421, In 1- 14: I am concerned that other processes than turbulence that govern the temperature are overlooked (at least it is not proven that they are negligible), i.e. advection and radiation divergence. For example, Savijarvi et al (2006) found rather strong impact of radiation divergence in stable boundary layers with low winds and with decoupling. Please comment.**

Response: We agree that as turbulence is unable to transport large amounts of heat or momentum in decoupled boundary layers, other transport processes such as radiation flux divergence will become relatively more important. However, the main focus of the analysis is the description of the external factors “curvature” and “temperature difference” on the turbulent fluxes and not a full assessment on all possible effects. We now mention however in the text that other things such as radiation balances may also change (especially in the field) and expect that these effects are extremely small over the length scales of our wind tunnel:

*Comparing wind tunnel with field experiments, we have to consider that in the field other meteorological processes such as radiation may also become important drivers for cold-air pooling and boundary layer decoupling. We expect, however, that these effects are extremely small over the length scales of our wind tunnel.*

**P5422, In 8-11: Figure 3 should be discussed in more detail.**

Response: we are aware that figure 3 is not easy to read but decided to keep the figure as the figure shows how the profiles are located within the cavity and over the flat surface. We think that the reader benefits from such an illustration. For a more concise description of the profiles we show the profiles in Figure 4 in high resolution. We now refer to Figure 3 more often.

**P5422: from section 3.3 the paper become less easy to follow since the abbreviations for the experiments (as E1, E2, etc) are less frequently used.**

Response: we revised the manuscript accordingly and now use the abbreviations throughout the paper.

**P 5422, In 25-29: The flux behaviour close the ground: please provide more evidence that the reduced flux magnitude towards the surface is not an effect of lacking statistics (too few robust measurements to make up a flux estimate). In addition, if these observations have been made in the roughness sublayer, I do expect the flux magnitude to increase with height. Could the authors provide some guidance whether the measurement were taken in the roughness sublayer, the surface layer or the boundary layer.**

Response: Please see our comments on the uncertainty above. Raupach et al. (1991) give roughness sublayer heights approximating  $2h$ , where  $h$  is the mean height of the roughness elements. Considering the low roughness lengths of snow the roughness sublayer would be below 1 cm. Since all measurements are above 1 cm above the surface, this means that measurements were not within the roughness sublayer. If we assume the boundary layer height to be 0.25 m in our wind tunnel (Clifton et al., 2006), then the lowest 10% of the boundary layer approximately are within the surface layer. This would mean the lowest 2.5



cm. Part of the lowest few points are within the surface layer and the rest are within the boundary layer. We added a note on the roughness sublayer to the text: *Assuming that all measurements are conducted above the roughness sublayer, then turbulent momentum and vertical turbulent heat fluxes within the stable internal boundary layer are expected to increase with decreasing distance to the snow surface* \citep{essery06}.

Clifton A, Rüedi JD, Lehning M (2006) Snow saltation threshold measurements in a drifting snow wind tunnel. *Journal of Glaciology* 52(179):585-596

**P5423, In 2: ....surface at X2 only ...**

Response: the peak is evident for X1 and X2. We changed the text to: *For low wind velocities, profiles of momentum fluxes feature a distinct peak approx. 0.03 - 0.04 m above the local surface for X1 and X2*(Figure 3, Figure 4).

**P5423, In 22-25: I only see support for this statement in Fig 4d.**

Response: we changed the text to be more clear here: *For higher wind velocities, however, the suppression of the vertical heat flux is confined to the lowest 0.01 - 0.02 m of the ABL and is much stronger for the downwind distance X2, where the maximum depth of the cavity is reached* (Figure 4d).

**P5424, In 7: explain in more detail what you expect here**

Response: we now clearly state what we want to discuss here: *As stated in the methods section, in neutrally stratified boundary layer flows, the main contributions to the Reynolds stress comes from sweep and ejection motions and both motions are nearly equal in their contribution* \citep{wallace}. *In the following, we will discuss the near-surface profiles resulting from our experiments with flows characterized by a changing atmospheric stability towards the surface. We particularly want to distinguish between turbulence phenomena observed for the flat and the concave setup.*

**P5424, In 16: ...of sweeps (Q4)...**

Response: changed accordingly.

**P5424, In 21: ... drainage flows...:** as mentioned above, I think the terms “low-level jet” and “drainage flow” are used quite loosely in the paper, so I have some reservations here that the suggested drainage flow is really a drainage flow. In this part of the analysis, the study could reveal a real drainage flow by repeating the experiment, but for an outer layer wind speed of 0 m/s. In that case the drainage flow would develop spontaneously.

Response: please see comments on major point 6) above.

**P5424, In 24-27: This result calls for an explanation, that is missing so far.**

Response: This is discussed in subsection *Discussion: Indications of boundary layer decoupling within the cavity*. We now refer to the following subsection in the text.

*The strong suppression of turbulent motions close to the surface is a clear indication for boundary layer decoupling at low wind velocities and will be discussed in the following section.*

**P5427, In 8: remove statement that “stability had a minor effect”**

Response: we changed the text, now reading: *While the stability had only a small effect on flow dynamics over the flat snow field, it strongly influenced the near-surface flow behavior over the concavely shaped snow patch, especially if the free-stream wind velocity was low.*

**P5427, In 27: “intermittently”: intermittent turbulence was not observed during the experiment, so this statement is somewhat suggestive.**

Response: we changed the sentence now reading: *Thus, for typical melt conditions of a seasonal snow cover, only the special experimental conditions with a concavely shaped snow patch and low free-stream wind velocities allowed the development of near-surface vertical profiles of turbulence that are typical for very stable regimes \citep{mahrt}, when the maxima of turbulence is reached in a layer decoupled from the surface.*

**P5428, In 11-17: It appeared to me somewhat surprising that at the end of the paper it appears that there are field data available to compare the tunnel experiments with. This would be very interesting to report.**

Response: there are different turbulence measurements available. Already published turbulence measurements at the Wannengrat test site indicated boundary layer decoupling for low wind velocities but measurements did not show if boundary layer decoupling is caused by wind velocity only or also due to the sheltering. Following that, these measurements were a motivation for wind tunnel experiments. We introduced a few sentences in the introduction part to clearly state this:

*Although measurements conducted by Mott et al. (2013) indicated that boundary layer decoupling over a melting snow patch especially occurred during low ambient wind velocities, the effect of the topography via sheltering could not be analysed. Furthermore, measurement results only gave a rough estimate on boundary layer dynamics close to the surface.*

**Figure 2: Caption: ....temperature (top) and wind velocity (bottom).....**

Response: we changed the figure accordingly.

**Figure 2: Please add error bars**

Response: Since the profiles are calculated from one experiment only we do not show an error bar. We show, however, profiles of mean and turbulent quantities including uncertainty estimates of each measurement point (see major comment above). Please see also the comment above regarding the repeatability of measurements and the error analysis for the turbulent quantities.

**Figure 3: This figure is not easy to read since the scale is at the bottom. In addition the figure is also very limitedly discussed in the text. Please rewrite and re-organize.**

Response: we are aware that figure 3 is not easy to read but decided to keep the figure as the figure shows how the profiles are located within the cavity and over the flat surface. We think that the reader benefits from such an illustration. For a more concise description of the profiles we show the profiles in Figure 4 in high resolution. We now refer to Figure 3 more often.

**Figure 3: label the panels a-d, and label on the right whether the plots refer to “E1” or “E2”.**

Response: we labelled panels a-d and also included E1 or E2 to the panels.

**Figure 3: Please add error bars:**

Response: Please see comment above - Error bars will not be included for flux profiles but we will show profiles of uncertainty estimates. Please refer to the general discussion of flux errors in the text.

**Figure 4: Please add error bars, and explain the colour labelling of the lines.**

Response: We added the labelling of the lines to Figure 4. Please see comments above for error bars.

**Figure 5 and 6: Please reconsider how useful are these plots. I mean I would not have expected something different than these fluxes being dominated by Q2 and Q4. Also add error bars.**

Response: Yes, it is not surprising that fluxes are dominated by sweeps and ejections. The results however underline the occurrence of boundary layer decoupling (nicely visible in the strong suppression of all local motions within the concave section at the lowest centimetres) for the E2V1 experiment despite rather low Richardson number. BUT what marks a clear difference to the distribution of quadrant motions for neutral flows is the clear dominance of sweeps at the height corresponding to the wind velocity height above the cold pool – that is shifted towards the surface for higher wind velocities.

**Figure 7: Labelling at top of panels like E2V1, E2V2 etc would be helpful.**

Response: Following your suggestion, we included labelling at top of panels.

**Figure 7: I do not see low-level jets in the bottom three rows, while manuscript suggests they are there. Please use a more objective way to define a “low level jet” or “wind maximum”.**

Response: please see my comment above.

**Figure 7: in the second row, the layer with the strongest wind shear coincides with a strong reduction in flux magnitude towards the surface. That is counterintuitive. Please add a vertical profile of Richardson number for a deeper insight. Figure 7 and 8: Please add error bars.**

Response: yes that is counterintuitive but is a direct result of boundary layer decoupling as it is now defined in the Introduction. We added Figure 8a to show the local Richardson number.

*We define boundary layer decoupling to be characterized by a suppression of turbulent mixing near the surface causing a significant reduction of vertical momentum transfer towards the ground (which would normally increase towards the surface where shear is strongest).*

*Response to Reviewer 2 (Richard Essery)*

We thank Richard Essery for his valuable comments. We answered below to all his comments. Reviewer's comments are in bold while our answers appear in normal font. Changes in the manuscript are shown in cursive.

**5414, 9 Momentum fluxes were also measured**

Response: we changed the text accordingly to: *Vertical profiles of sensible heat and momentum fluxes*

**5414, 15 Clarify in what sense “drainage flows were decoupled from the surface”**

Response: Following the comments from Reviewer 1 we do not call the wind speed maximum a drainage flow anymore. We changed the corresponding paragraph to: *For those conditions, the near-surface suppression of turbulent mixing was observed to be strongest and the ambient flow was decoupled from the surface enhancing near-surface atmospheric stability over the single snow patch.*

**5415, 9 A missing reference here: Liston, G. E. (1995). Local advection of momentum, heat and moisture during the melt of patchy snow covers. Journal of Applied Meteorology, 34, 1705-1715.**

Response: we added the missing reference.

**5415, 15 Burns and Chemel**

Response: we changed Bruns to Burns.

**5416, 15 Perhaps more importantly, high vertical resolutions are required**

Response: Yes, the reviewer is right. We changed the sentence accordingly: *Applying Large-Eddy Simulations, a high horizontal resolution of at least 5 m and near-surface vertical resolution of less than 1 m are necessary to adequately represent the formation of thermal internal boundary layers.*

**5416, 25 It is fairly obvious, but neither z nor delta have been defined.**

Response: Yes, we changed the sentence to: ... *(normalizing the vertical measurement resolution (dz) by boundary layer height (delta) in the wind tunnel (dz/delta) this means 0.016).*

**5417, 26 Make it clear that the depth of the concavity is being discussed, not the depth of the snow.**

Response: To be more clear here we changed the sentence to: *The cavity has a length (\$L\$) of 1.6 m and a maximum depth (\$z\_{max}\$) of 0.1 m (Figure 1).*

**5418 Z0 is a redundant quantity, being 0 by definition (and might be confused with z\_0 by boundary-layer meteorologists). I think it would be more clear to have z=0 redefined for each experiment to be the snow surface in E1 or the highest point of the concave surface in E2. How much did the surface change during the experiment, and is it reasonable to assume that most of the melt occurred between rather than during the measurement periods? Why were the measurement periods different for E1 and E2?**

Response: Yes, we agree with the reviewer and changed the wording and definition throughout the paper and changed all figures accordingly: *All heights are given relative to z=0, which is the height of wooden floor and the initial snow cover at fetch distance 0. For the concave setup, z=0 corresponds to highest point of the cavity.*

**5419, 3 Exceeding what threshold?**

Response: we changed the text to: *If a time-series was influenced by natural convection for more than 10% of the time, data were not considered for the following analysis.*

**5419, 9-13 This sentence and Table 2 contain exactly the same information; one of them is redundant.**

Response: yes, we extended and revised the description in the text and skipped table 2: *The resulting types of motions are following the description in Table 1: outward motion of high-momentum fluid (Q1), ejections of low-momentum fluid (Q2), wallward motion of low momentum fluid (Q3) and sweeps of high-moment fluid towards the wall (Q4).*

**5419, Equation (1) Either subscripts or conditions are required in the integral to pick out the quadrants.**

Response: We have added subscripts

$$\langle u'v' \rangle_{i,H} = \lim_{T \rightarrow \infty} \frac{1}{T} \int_0^T u'(t)v'(t)I_{i,H}[u'(t)v'(t)]dt$$

where  $T$  is the length of the time-series and  $I_{i,H}$  is a function that triggers the events that are larger than the root mean square of the single components multiplied by  $H$  as follows:

$$I_{i,H}[u'(t)v'(t)] = \begin{cases} 1 & \forall (u', v') \in Q_i \\ 0 & \text{otherwise} \end{cases}$$

The four quadrants are defined as follows:

Quadrant 1 - outward interactions:  $u' > 0, v' > 0 \rightarrow (u', v') \in Q_1$

Quadrant 2 - ejections:  $u' < 0, v' > 0 \rightarrow (u', v') \in Q_2$

Quadrant 3 - inward interactions:  $u' < 0, v' < 0 \rightarrow (u', v') \in Q_3$

Quadrant 4 - sweeps:  $u' > 0, v' < 0 \rightarrow (u', v') \in Q_4$

**5420, 9 Table 1 shows ambient temperatures ranging between 8.5 and 14.0 C.**

Response: we thank the reviewer for that hint. We changed the text accordingly.

**5421, 19 It takes some faith to see “a distinct local wind maximum” in the profiles for E2V1, particularly without an estimate of the uncertainty in the measurements.**

Response: as discussed above, we included an uncertainty estimation. Regarding the wording “a distinct local wind maximum” we skipped distinct.

**Table 1 What heights were used in calculating the bulk Richardson numbers? I couldn't make sense of the values. V in the caption is U elsewhere. Theta in the table is T elsewhere (and it isn't potential temperature). The labels “c = concave, f = flat” are no used.**

Response: we changed Table 1 to be consistent with labels used in the manuscript.

**Figure 3 Is there any advantage to having X1 and X2 profiles on the same plots? Splitting them would remove the need for the complicated and confusing axes.**

Response: we are aware that figure 3 is not easy to read but we have decided to keep the figure as it shows how the profiles are located within the cavity and over the flat surface. We think that the reader benefits from such an illustration. For a more concise description of the profiles we show the profiles in Figure 4 in high resolution. We now refer to Figure 3 more often.

**Figure 4 Theta in the caption is T in the figure**

Response: The reviewer is right that Theta should read T. We changed the caption for Figures 3 and 4.

# Wind tunnel experiments: Cold-air pooling and atmospheric decoupling above a melting snow patch

Rebecca Mott<sup>1</sup>, Enrico Paterna<sup>1</sup>, Stefan Horender<sup>1</sup>, Philip Crivelli<sup>1</sup>, and Michael Lehning<sup>1,2</sup>

<sup>1</sup>WSL Institute for Snow and Avalanche Research SLF, Davos, Switzerland

<sup>2</sup>School of Architecture, Civil and Environmental Engineering, Laboratory of Cryospheric Sciences (CRYOS), École Polytechnique Fédérale de Lausanne, Lausanne, Switzerland

*Correspondence to:* Rebecca Mott  
(mott@slf.ch)

**Abstract.** The longevity of perennial snow fields is not fully understood but it is known that strong atmospheric stability and thus boundary layer decoupling limits the amount of (sensible and latent) heat that can be transmitted from the atmosphere to the snow surface. The strong stability is typically caused by two factors, i) the temperature difference between the (melting) snow surface and the near-surface atmosphere and ii) cold-air pooling in topographic depressions. These factors are almost always a prerequisite for perennial snow fields to exist. For the first time, this contribution investigates the relative importance of the two factors in a controlled wind tunnel environment. Vertical profiles of sensible heat and momentum fluxes are measured using two-component hot wire and one-component cold-wire anemometry directly over the melting snow patch. The comparison between a flat snow surface and one that has a depression shows that atmospheric decoupling is strongly increased in the case of topographic sheltering but only for low to moderate wind speeds. For those conditions, the near-surface suppression of turbulent mixing was observed to be strongest and the ambient flow was decoupled from the surface enhancing near-surface atmospheric stability over the single snow patch.

## 1 Introduction

Snow cover can be highly heterogeneous on various scales, introducing inhomogeneities in surface characteristics such as surface albedo, roughness or temperature (Essery, 1997). Once an alpine snow cover gets patchy in spring, steps in surface roughness and surface temperature induce the development of thermal internal boundary layers. Increasing air temperatures in spring cause stable internal atmospheric layers above the melting snow-covered surface. The stability is further en-

hanced by the forced flow of warm air advected by the mean wind from the snow-free land over the colder snow-covered areas changing the atmospheric boundary layer characteristics over snow by increasing the local air temperature there. The complex interactions between snow, bare ground and atmosphere strongly affect the energy balance at the snow surface, thus snow melt and runoff  
25 in spring. Typically, hydrological and energy balance studies do not account for those processes involved because they rely on the existence of constant flux layers and simply apply bulk transfer models. Only a small number of investigations on processes driving snow melt that are affected by the development of thermal internal boundary layers exist so far (Liston, 1995; Essery , 1997; Neumann and Marsh, 1998; Essery et al., 2006; Granger et al., 2006; Mott et al., 2013, 2015).

30 Another phenomenon that is directly linked to the existence of stable internal boundary layer development is the formation of cold-air pools driving the survival of perennial snow fields (Fujita et al., 2010). Cold air pools typically develop in closed sink holes, topographical depressions or narrow valleys (Whiteman et al., 2001; Vosper et al., 2014). They either develop due to drainage flows (Whiteman et al., 2008; Bodine et al., 2006) or due to sheltering effects (Gustavsson et al.,  
35 1998; Burns and Chemel, 2014). Sheltering effects and in situ cooling are typically described for small-scale valleys (i.e. 100 m deep and up to 3 km wide), where the valley air is decoupled from the atmospheric boundary layer above due to the sheltering effect of valley geometry (Price et al., 2011). Sheltering causes reduced turbulence and prevents heat transfer from above, allowing the valley atmosphere to cool by radiative heat loss (Burns and Chemel, 2014). The sheltering effect is  
40 enhanced by strong atmospheric stabilities that are typically connected with calm wind conditions and boundary layer decoupling (suppression of turbulence near the surface) is promoted (Vosper et al., 2014). Cold-air pooling can also occur over snow fields that are located within topographical depressions where associated atmospheric decoupling is mainly driven by the cooling effect of the underlying snow on the air. This phenomenon, however, has gained little attention so far (Fujita et  
45 al., 2010). Long-lasting snow patches are typically located within topographical depressions because snow is preferentially accumulated in sheltered areas (Tabler, 1975; Winstral et al., 2002; Lehning et al., 2008; Mott et al., 2010; Dadic et al., 2010; Mott et al., 2014) and the snow is well protected within topographical depressions due to lower wind speeds decreasing turbulent fluxes (Mott et al., 2011a). For low wind speeds, the cooling effect of the snow and advective transport of warm air  
50 increase the local atmospheric stability and promote cold-air pooling and atmospheric decoupling above snow patches (Fujita et al., 2010; Mott et al., 2013).

The mean perimeters of snow patches in alpine terrain are typically in the range of tens to hundreds of meters. The formation of shallow cold-air pools and connected atmospheric decoupling above small-scale snow patches is difficult to measure or to simulate with a numerical model (Mott  
55 et al., 2015). In the field, atmospheric profiles obtained from eddy-correlation measurements are typically based on a few measurement points, which makes it difficult to capture boundary layer dynamics of shallow internal thermal boundary layers. Especially turbulent heat fluxes close to the



snow surface are difficult to measure in the field because of the relatively large path lengths of sonic anemometers and consequentially the low vertical resolution of measurement points close to the surface. Although measurements conducted by Mott et al. (2013) indicated that boundary layer decoupling over a melting snow patch especially occurred during low ambient wind velocities, the effect of the topography via sheltering could not be analyzed because varying one parameter at a time is difficult if not impossible to accomplish in the field.

Applying Large-Eddy Simulations, a high horizontal resolution of at least 5 m and near-surface vertical resolution of less than 1 m are necessary to adequately represent the formation of thermal internal boundary layers. What cannot be captured with that resolutions is the strong suppression of turbulence due to strong atmospheric stability at the lowest centimeters above the snow surface (Mott et al., 2015). Wind tunnels provide controlled conditions to measure the boundary layer dynamics above cooled surfaces (Ohya, 2001; Ohya et al., 2008). Furthermore, the available measurement techniques also allow us to measure vertical profiles of turbulent quantities with a high vertical resolution of approximately 0.005 m (normalizing the vertical measurement resolution ( $dz$ ) by boundary layer height ( $\delta$ ) in the wind tunnel ( $dz/\delta$ ) this means 0.016). This comes at the expense of reduced eddy sizes and directional variation of winds in the tunnel. Measurements conducted in the wind tunnel are thus expected to advance our understanding of the flow field development and the associated heat exchange when the flow crosses a single snow field. Earlier wind-tunnel studies of the atmospheric stable boundary layer were conducted using a thermally stratified wind tunnel (Ohya, 2001; Ohya et al., 2008). For those experiments, stably stratified flows were generated by heating the wind tunnel airflow and cooling the test-section floor, creating high temperature differences between air and floor up to  $40^{\circ}C$  and bulk Richardson numbers larger than 1. In our experiments, the warmer air within the wind tunnel flows across a snow patch creating a shallow stable layer with smaller temperature differences up to  $14^{\circ}C$ , which are typical for spring conditions when snow melts in higher altitudes (Mott et al., 2011a).

In this experimental study we investigate the development of the atmospheric boundary layer when the boundary layer flow crosses a single snow patch. The purpose of this study is to examine boundary conditions for cold-air pooling and atmospheric boundary layer decoupling over seasonal snow patches or perennial snow fields. We define boundary layer decoupling to be characterized by a suppression of turbulent mixing near the surface causing a significant reduction of vertical momentum transfer towards the surface (which would normally increase towards the surface where shear is strongest). The experimental setup accounts for the effect of synoptic wind forcing and the effect of the topography. With this setup we want to look into the relative role of topographic sheltering versus temperature differences in the generation of decoupling and stratification over snow patches.

## 2 Methods and Data

### 2.1 Experimental methods

95 All experiments conducted for that study are listed in Table 1. Measurements were performed in the  
SLF boundary layer wind tunnel (Figure 1) in Davos in a non-heated building at 1650m a.s.l.. The  
wind tunnel is an open-circuit suck-down type and 17 m long and has a cross section of 1x1m. In the  
upwind part of the wind tunnel the boundary layer flow was preconditioned by spires and additional  
roughness elements, that were arranged along a 6 m long fetch. In the middle section 6.4 m of  
100 wooden plates featured a smooth surface. The measurement section was located at the downwind  
end of the wind tunnel, consisting of a 1.6 m long snow patch. The snowpack was isothermal during  
all experiments. The surface shape of the snow patch was either flat (Experiment E1) or concave  
(Experiment E2). The cavity has a length ( $l$ ) of 1.6 m and a maximum depth ( $z_{max}$ ) of 0.1 m (Figure  
1). These dimensions ( $z_{max}:l=0.06$ ) were defined to scale with a cavity in the Wannengrat catchment  
105 ( $z_{max}:l=2.5:60=0.04$ ), that was studied by Mott et al. (2013) revealing boundary layer decoupling  
above a melting snow field. For experiments E1 and E2 profiles of mean and turbulent quantities  
were measured at 0.4 m (X1) and 0.8 m (X2) downwind of the leading edge of the snow patch. For  
E2, the depth of the snow-covered depression is 0.06 m at X1 and 0.1 m at X2. All experiments were  
performed at free-stream wind velocities of approximately 1, 2 and 3  $m.s^{-1}$  (V1,V2,V3). All heights  
110 are given relative to  $z=0$ , which is the height of wooden floor and the initial snow cover at fetch  
distance 0. For the concave setup,  $z=0$  corresponds to highest point of the cavity. Consequently, for  
the concave setup E2 the snow surface belongs to  $z=-0.06$  m at X1 and to  $z=-0.1$  m at X2. Please  
note that due to the configuration of the probes, we were able to measure closer to the ground for the  
flat setup (E1) than for the concave setup (E2). While the lowest measurement point above snow is  
115 approximately 0.002 m for E1 it is 0.01 m for E2. Furthermore, the snow surface temperature was  
at its melting point during the whole experiment, resulting in a change of the snow surface during  
the experimental period. As a consequence of the melting snow surface, the heights above the snow  
surface are not consistent throughout the experimental period. Thus, not only profiles of E2, but also  
of E1V2 and E1V3 feature negative heights.

120 The temperature and velocity fluctuations were measured simultaneously using a system of a  
two-component platinum coated hot-wire anemometer (TSI 1240-60) and a one-component cold-  
wire anemometer (Dantec 55P11). The calibration was performed in situ before each test against a  
calibrated miniature fan anemometer (Schiltknecht MiniAir20) for the velocity measurements and  
against a digital thermometer (Labfacility Tempmaster-100). To ensure high statistical stationarity  
125 of the fluxes we designed our experiments by sampling the flow at least hundred times the integral  
time scale (Tropea et al., 2007). Data were acquired at a frequency of 1 kHz and for 100 s during  
the tests on setup 1 and 20 s during the tests on Experiment 2 (E2). The data were low-pass filtered  
by means of a butterworth filter with a cut-off frequency of 100Hz. Furthermore, to eliminate low-

frequency trends in the signal data were also high-pass filtered with a cut-off frequency of 0.2 Hz.

130 Being the tests conducted at low velocities a threshold was applied based on the Reynolds (the ratio of momentum forces to viscous forces) and Grashof number (the ratio of the buoyancy to viscous forces) to eliminate velocity data significantly influenced by natural convection of the wire (Collis and Williams, 1958). The time-series exceeding the latter threshold for more than 10% of the time were not considered for the following analysis. Following this procedure four points in total have  
 135 been removed from the data set. To account for the slope at measurement location X1 we applied the planar fit approach following Wilczak et al. (2001).

We estimated the uncertainty, considering both the systematic and random components. The random uncertainty is significantly larger than the systematic uncertainty. The random uncertainty of a variable  $q$  was considered as follows:

$$140 \quad u_q = \sigma_q / (\langle q \rangle \sqrt{N}) \quad (1)$$

with  $\sigma$  the standard deviation,  $N$  the number of independent samples separated by the integral-time scale of  $u$ . We did not appreciate significant differences applying the method of Mann and Lenschow (1994), therefore we adopted the simplest method. We spatially averaged the total uncertainty (systematic and random) within the first 0.1 m from the snow surface where turbulent mixing is mainly  
 145 occurring. The uncertainties of the mean streamwise velocity and temperature fall below 3.5%. The uncertainties of the fluxes are larger and between 9% and 33%. The large uncertainties of the fluxes reflect the high level of turbulence in the flow together with the mean values approaching to zero towards the surface.

## 2.2 Quadrant analysis

150 Quadrant analysis consists of conditionally averaging the shear stresses into four quadrants depending on the sign of the streamwise and vertical velocity fluctuations (Wallace et al., 1972).

If  $u$  and  $w$  correspond to streamwise and vertical velocity and primes indicate the deviation from the average value, each quadrant event  $\langle u'w' \rangle_i$  can be defined as:

$$\langle u'w' \rangle_i = \lim_{T \rightarrow \infty} \frac{1}{T} \int_0^T u'(t)w'(t)I_i[u'(t)w'(t)]dt \quad (2)$$

155 where  $T$  is the length of the time-series, and  $I_i$  is a function that triggers of a specific quadrant  $Q_i$ :

$$I_i[u'(t)w'(t)] = \begin{cases} 1 & \text{if } (u'w') \in Q_i \\ 0 & \text{if } (u'w') \notin Q_i \end{cases} \quad (3)$$

The resulting types of motions are the following: outward motion of high-momentum fluid (Quadrant 1), ejections of low-momentum fluid (Quadrant 2), wallward motion of low momentum fluid

160 (Quadrant 3) and sweeps of high-moment fluid towards the wall (Quadrant 4). The four quadrants  
are defined as follows:

Quadrant 1 (Q1):  $u' > 0, v' > 0 \rightarrow (u', v') \in Q1$

Quadrant 2 (Q2):  $u' < 0, v' > 0 \rightarrow (u', v') \in Q2$

Quadrant 3 (Q3):  $u' < 0, v' < 0 \rightarrow (u', v') \in Q3$

165 Quadrant 4 (Q4):  $u' > 0, v' < 0 \rightarrow (u', v') \in Q4$

While Q1 and Q3 motions are positive stress producing motions, ejections and sweeps contribute positively to the Reynolds stress. The negative contributions by Q1 and Q3 motions corresponds to the interaction between ejection and sweep motions. In neutrally stratified boundary layer flows, the  
170 main contributions to the Reynolds stress comes from sweep and ejection motions and both motions are nearly equal (Wallace et al., 1972).

In our case all the events from each quadrant are considered and no event is discarded based on its magnitude. Therefore the analysis concentrates on the overall flow dynamics rather than focusing on the strength of the motions. The second (ejections) and fourth (sweeps) quadrants constitute a  
175 positive contribution to the production of turbulent kinetic energy and to the momentum flux towards the surface, while the other two constitute a negative contribution.

### 3 Results

#### 3.1 Experimental conditions

The flow conditions for each experimental case are listed in Table 1. The free-stream wind velocity  $U_\infty$  ranged between 0.9 and 3.3  $ms^{-1}$  with ambient air temperatures ranging between 8.5 and  
180 14.0  $^{\circ}C$ . The snow surface temperature was 0 $^{\circ}C$  for all experiments. Since, the flow first crossed a smooth wooden floor before crossing a flat (E1) or concavely shaped (E2) snow patch, the flow was streamwise inhomogeneous. The bulk Richardson numbers, defined as a dimensionless number relating vertical stability and vertical shear, are below the critical value of 0.25 for all profiles.  
185 That means that the flow is expected to be dynamically unstable and turbulent. For both setups, the bulk Richardson number ( $Ri_{bulk}$ ) was slightly higher at X2 than at X1 due to a slightly stronger cooling of the atmosphere further downwind. While the flow for the experimental cases with low free-stream wind (V1) was statically stable with  $Ri_{bulk}$  numbers ranging between 0.19 and 0.22, experimental cases driven by higher free-stream wind velocities (V2,V3) show low  $Ri_{bulk}$  numbers  
190 ranging between 0.02 and 0.05.

#### 3.2 Vertical profiles of mean quantities

The vertical profiles of the streamwise wind velocity  $U$  and mean air temperature  $T$  are illustrated in Figure 2 for the different experimental cases and fetch distances. The mean air temperature is

normalized by the difference between the ambient air temperature  $T_\infty$  and the surface temperature  
195  $T_s$  (which was  $0^\circ C$  throughout the measurements). The mean wind velocity  $U$  is normalized by the  
free-stream wind velocity  $U_\infty$ .

The temperature profiles show stably stratified flows, that are generated above the snow patch at  
fetch distances of X1 and X2. The stable layers are deeper for the concave setup ( $E2$ ) than for the flat  
setup ( $E1$ ). The decrease in air temperature close to the surface is considerably stronger for  $E1$  than  
200 for  $E2$ , resulting in a stronger local atmospheric stability close to the wall. We have to note, however,  
that no measurement points are available at the lowest 0.01 m above the surface ( $z < -0.09$  m) for  
 $E2$ . We expect that a higher near-surface measurement resolution for  $E2$  would probably reveal an  
enhanced temperature gradient below  $z = -0.09$  m, at least similar to what we observed for  $E1$  where  
the highest temperature gradient was found below  $z = 0.01$ . Over the flat snow patch, the near-surface  
205 air temperature gradient is higher at X1 than at X2. Over the concave snow patch, the near-surface  
air temperature gradient increases in downwind direction revealing colder air at the lowest point of  
the concave. The thermal boundary layer grows in downwind direction and is deeper for lower wind  
velocities and for the concave setup.

The velocity profiles of  $E1$  show a weakly pronounced local wind velocity maximum formed at  
210 X2 for low free-stream wind velocity ( $E1V1$ ). For higher free-stream wind velocities ( $E1V2$ ,  $E1V3$ ),  
the profiles exhibit a gradually increasing wind velocity with height without a local maximum evi-  
dent. The near-surface wind velocities are slightly higher at X2 than at X1. Wind profiles of  $E2$  show  
a local wind maximum for the low wind velocity case  $E2V1$  and less pronounced for  $E2V2$ . For ex-  
periments with high free-stream wind velocities ( $E2V3$ ), the formation of the local wind maximum  
215 is not evident anymore. For  $E2V1$ , the wind profile at X1 shows a local wind maximum at  $z = -0.025$   
m (0.035 m above the local surface). At X2, the wind maximum was measured at  $z = -0.05$  m (which  
corresponds to 0.05 m above the local snow surface). The low-level maxima in velocity might be  
caused by the acceleration of the flow behind the topographical step (the highest point of the cavity)  
due to the detachment from the surface. A deep layer of strong wind velocity gradient is visible  
220 below the peak of wind velocity. Close to the wall, wind velocities become very small (smaller than  
0.2 m/s) and are much smaller for both distances than measured over the flat snow patch ( $E1$ ) for a  
similar ambient wind velocity. The extremely low values of wind velocities within the cavity for the  
low wind velocity case indicates boundary layer decoupling there. The temperature profiles for the  
low wind velocity cases are two-layered and show a change of temperature gradient at the height of  
225 the respective peaks in wind speed. Similar to the low wind velocity case, temperature profiles of the  
high wind velocity cases show a strong layering that coincides with the wind velocity profile.

### 3.3 Vertical profiles of turbulent quantities

Figure 3 illustrates vertical profiles of turbulent momentum flux and vertical turbulent heat flux  
along the snow patch for the flat and the concave setup. Fluxes are normalized by the free-stream

230 wind velocity and temperature difference between snow surface and ambient air. Figure 4 zooms in  
on the near-surface profiles (ranging from  $z=-0.1$  to  $+0.06$  m) of turbulent momentum and vertical  
turbulent heat flux for the low wind velocity case V1 and the high wind velocity case V3. Primes  
' indicate the deviation from the mean value and overbars the average. Momentum fluxes are thus  
235 computed as a covariance between instantaneous deviation in horizontal wind speed ( $u'$ ) from the  
mean value ( $\bar{u}$ ) and instantaneous deviation in vertical wind speed ( $w'$ ) from the mean value ( $\bar{w}$ ).  
Vertical heat fluxes are computed as a covariance between instantaneous deviation in air temperature  
( $T'$ ) from the mean value ( $\bar{T}$ ) and instantaneous deviation in vertical wind speed ( $w'$ ) from the mean  
value ( $\bar{w}$ ). In theory a thermal internal boundary layer develops with increasing depth in downwind  
distance as a neutrally stratified flow crosses a single snow patch. Assuming that all measurements  
240 are conducted above the roughness sublayer, then turbulent momentum and vertical turbulent heat  
fluxes within the stable internal boundary layer are expected to increase with decreasing distance to  
the snow surface (Essery et al., 2006).

For experiments conducted over the flat snow patch E1, profiles reveal an increase of negative  
momentum fluxes with decreasing distance to the snow surface (Figure 3 a, Figure 4a, c). Contrary,  
245 the vertical profiles of turbulent quantities for the concave snow patch (Figure 3 c, Figure 4a, c) show  
a distinct maximum in the negative vertical momentum flux at the height of the shear layer indicating  
that both, the surface and the high-shear region around  $z=0$  contribute to turbulence generation. For  
low wind velocities, profiles of momentum fluxes feature a distinct peak approx. 0.03 - 0.04 m above  
the local surface for X1 and X2 (Figure 3 c, Figure 4 a, c). Below that maximum, momentum fluxes  
250 strongly decrease towards the snow surface. This near-surface suppression of momentum flux is  
strongest further downwind at X2, at the maximum depth of the cavity. The peak of the momentum  
flux appears to be strongest at the first measurement location downstream of the fetch transition  
(X1). At the downwind location X2, however, the magnitude of the momentum flux is much lower  
for the whole profile.

255 At X1 profiles of the vertical turbulent heat flux reveal a local maximum at  $z=+0.02$  m for the  
flat snow patch with a decrease towards the surface below that maximum (Figure 3 b and Figure  
4 c, d). Further downwind, the maximum heat flux was measured at the lowest point above the  
surface ( $z=+0.002$  m) and no suppression of the vertical turbulent heat flux was measured there.  
On the contrary, for the concave setup, all profiles of heat fluxes feature a similar shape revealing  
260 distinct peaks of fluxes at the lowest few centimeters of the atmospheric layer (0.02-0.04 m above  
the local surface) coinciding with the maximum in vertical velocity fluctuations (not shown). Below  
that maximum, fluxes strongly decrease towards the snow surface (Figure 3 d and Figure 4). The  
maximum can be found at a higher distance to the ground for the low wind velocity case E2V1,  
coinciding with maximum wind speed at a height of 0.04 - 0.05 m above the local snow surface and  
265 strong shear below the local wind maximum (Figure 2, Figure 4). Close to the surface, the fluctuation  
of streamwise and vertical velocity fluctuations are rapidly suppressed at both downwind distances

and for all wind velocities. For higher wind velocities, however, the suppression of the vertical heat flux is confined to the lowest 0.01 - 0.02 m of the ABL and is much stronger for the downwind distance X2, where the maximum depth of the cavity is reached (Figure 4d).

### 270 3.4 Turbulence phenomena at the snow surface

Results from the quadrant analysis are presented for the flat setup *E1* (Figure 5) and the concave setup *E2* (Figure 6). The stress fraction contribution of each quadrant gives insight into the physics of turbulence structures close to the wall (snow cover).

As stated in the methods section, in neutrally stratified boundary layer flows, the main contribu-  
275 tions to the Reynolds stress comes from sweep and ejection motions and both motions are nearly equal in their contribution (Wallace et al., 1972). In the following, we will discuss the near-surface profiles resulting from our experiments with flows characterized by a changing atmospheric stability towards the surface. We particularly want to distinguish between turbulence phenomena observed for the flat and the concave setup. For *E1* the ejections (Q2) and sweeps (Q4) are observed to dominate  
280 the other two events over the whole boundary layer depth (Figure 5). Both contributions increase with decreasing distance to the wall promoting the downwards directed momentum flux. This result is consistent for all free-stream wind velocities (i.e. experiments *E1V1*, *E1V2*, *E1V3*). This distribution is analogous to the distribution of quadrant motions in neutrally stratified boundary layer flows over flat surfaces, where the ejection-sweep cycle was observed to be induced by coherent flow  
285 structures (Adrian et al., 2000).

Over the concave snow patch *E2*, ejections and sweeps are observed to dominate over the other two quadrant motions, similarly to the flat case (Figure 6). In contrast to *E1*, profiles for *E2* reveal a clear dominance of sweeps (Q4) of high speed fluid downward directed close to the snow surface for all setups, in particular for the lowest wind velocity case *E2V1* where larger stability is also observed  
290 (Figure 6). This marks a clear difference with the distribution of quadrant events for boundary layer flows in neutral stability conditions (see Methods section). At the lowest velocity it is interesting to observe that the peak of both ejections (Q2) and sweeps (Q4) (i.e. the height of peak wind velocity) occurs at a significantly higher distance from the snow surface than in case of the two other tests at higher velocity. The strong suppression of turbulent motions close to the surface is a clear indication  
295 for boundary layer decoupling at low wind velocities and will be discussed in the following section.

## 4 Discussion: Indications of boundary layer decoupling within the cavity

In order to discuss the near-surface turbulence in more detail we show the near-surface profiles of mean wind velocity, the vertical momentum and heat fluxes as well as the shear stress distribution for the low and high wind velocity cases at the different measurement locations (Figure 7). Figure  
300 8 shows the gradient Richardson number calculated from local wind and temperature gradients for

atmospheric layers (height of layers is 0.025 m) and the Reynolds number calculated from the local wind velocity at the respective measurement point for experiments *E2V1* and *E2V3*.

For the low wind velocity case *E2V1*, sweeps of high-speed fluid appear to be more decoupled from the surface of the cavity at X2 showing the local wind maxima at a higher level at  $z=-0.05$  m corresponding to the peak of ejections (Q2) and sweeps (Q4) (Figure 7 e, h). These strong local motions efficiently transport momentum and heat at the height of the local wind maximum (Figure 7f, g). The region below this local flow acceleration corresponds to a region of reduced turbulent mixing as observed in the vertical profiles of heat and momentum flux (Figure 7f, g). The rapid decrease of all strong local motions below the peak at  $z=-0.05$  m further confirms a strong suppression of turbulent mixing, thus strong atmospheric decoupling over the deepest point of the concave. Boundary layer decoupling is also revealed by the high gradient Richardson numbers for those points within the cavity, clearly exceeding the critical value of 0.25 only for the low wind velocity case (Figure 8a). Furthermore, very low Reynolds numbers calculated for measurement points below  $z=-0.05$  m that are significantly lower than for the higher wind velocity case indicate laminar flow close to the surface (Figure 8b). These profiles suggest that the higher stability at X2 at the lowest velocity forces the unsteady and coherent flow structures to develop above the cold pool. Moreover, in this latter case such strong reduction of ejections (Q2) and sweeps (Q4) in the decoupled region to the level of the other two quadrant events causes the vertical momentum flux to reduce toward zero (Figure 7f). The strong suppression of high-momentum fluid from the outer region and the strong suppression of turbulent mixing close to the wall (Figure 8) indicates favorable conditions for cold-air pooling within the cavity, which is strongest at the maximum depth of the cavity (Figure 7 f, g).

For the higher wind velocity cases *E2V2* and *E2V3*, the peak of contributions by Q2 and Q4 motions is shifted towards the wall and the suppression of turbulence is less pronounced and confined to the lowest 0.02 m of the ABL. Over the maximum depth of the cavity, at X2, the peak of Q2 and Q4 motions involve a 0.03 m deep layer of enhanced turbulent mixing (Figure 7 o, p). Thus, with increasing wind velocity gradients towards the wall, sweeps become more dominant towards the snow surface (dominant motion at the lowest points) indicating the rush-in of high speed fluid of the outer layer into the wall region. Furthermore, the strong contribution of Q1 is very conspicuous at X2 and show high values close to the wall. This strong increase of outward interactions (Q1) which are observed to increase with the free-stream velocity (Figure 7l, p) is a further clear departure from the commonly observed distribution of quadrant motions in neutrally stratified boundary layer flows. The positive streamwise fluctuations, given by the Q1 and Q4 events, dominate the flow especially at the highest free-stream velocities (Figure 7p). This is due to sweeps (Q4) towards the near-surface region as discussed above, and to the resulting displacement of high speed, colder fluid upwards (Q1) from the near-surface region as an effect of the stronger mixing occurring at the higher velocities. The outward interactions (Q1) can be therefore seen as bouncing flow resulting from preceding sweeps (Q4) directed towards the snow surface. This finds confirmation from the observation at the higher



tested free-stream velocity  $E2V3$  where the sweeps (Q4) are peaking closer to the snow surface, and by the relatively higher outward interactions (Q1) at X2 where the concave section allows the cold pool to form and as a consequence the mixing process to be stronger at the highest velocities. Thus, the inertial forces appear to be strong enough to mix most of the boundary layer within the cavity causing an enhancement of turbulent fluxes of momentum and heat close to the wall. At the deepest point of the cavity, however, the turbulent mixing is still suppressed within a very shallow layer at the wall and the concave surface still allows cold-air pooling.

These experiments were conducted for meteorological conditions typically observed over patchy snow covers, when the temperature difference between the snow surface and the ambient air typically ranges up to  $15^{\circ}C$  causing low bulk Richardson numbers ( $Ri_b < 0.25$ ) meaning that the flow is dynamically unstable. Wind tunnel studies performed by Ohya (2001) and Ohya et al. (2008) over a flat cooled surface demonstrated that a significantly stronger bulk atmospheric stability (Richardson number larger than 1) results in a suppression of momentum and heat fluxes over the whole boundary layer depth. In contrast to Ohya (2001); Ohya et al. (2008), our wind tunnel study shows that close to the surface the local gradient Richardson number clearly exceeds the critical Richardson value, but only for calm wind conditions and within sheltered locations, when buoyancy effects start to dominate over turbulence generation by shear. Thus, for typical melt conditions of a seasonal snow cover, only the special experimental conditions with a concavely shaped snow patch and low free-stream wind velocities allowed the development of near-surface vertical profiles of turbulence that are typical for very stable regimes (Mahrt, 2014), when the maxima of turbulence is reached in a layer decoupled from the surface. For high free-stream wind velocities, the inertia of the flow becomes strong enough to mix the boundary layer above the snow surface (also for concave setup) and to consequently inhibit the stagnation of cold air and associated boundary layer decoupling within the local depression.

Comparing the flux profiles of the different experiments and at different locations, we have to note that the locations measured at the downwind locations X1 and X2 will have varying footprints for the fluxes depending on wind speeds. At the same time, the differences between profiles at X1 and X2 give a first indication of how fluxes change in the streamwise direction. It is clear that lateral transport of heat and momentum plays an important role for the given conditions and that the net effect of a topographic depression on the boundary layer above still needs to be systematically analyzed.

The experimental results confirm the field study performed by Mott et al. (2013) who observed a strong suppression of downward heat fluxes close to the snow surface during calm wind conditions indicating boundary layer decoupling. The measurements of Mott et al. (2013) were, however, only conducted over a concavely shaped snow patch and lacked simultaneous measurements over a flat snow patch. Furthermore, measurements of the vertical profiles of turbulence intensities that were conducted by an eddy-correlation system were restricted by the low possible number of three measurements points. Compared to field measurements, the experimental setup in the wind tunnel

375 allowed a high vertical resolution of flux measurements and allowed us to account for the effect of  
the topography on the flow development and the generation of turbulence in atmospheric layer adja-  
cent to the snow. Comparing wind tunnel with field experiments, we have to consider that in the field  
other meteorological processes such as radiation may also become important drivers for cold-air  
pooling and boundary layer decoupling. We expect, however, that these effects are extremely small  
380 over the length scales of our wind tunnel.

## 5 Conclusions

Wind tunnel experiments on flow development over a melting snow patch were conducted for me-  
teorological conditions typically observed over patchy snow covers and strong snow melt in alpine  
environments. For the first time wind tunnel experiments were conducted over a snow field to explore  
385 the relative role of topography versus pure thermo-dynamics in causing atmospheric decoupling for  
melting snow conditions. The experiments give evidence that topography is critical for the process  
of atmospheric decoupling by significantly altering the near-surface flow field due to sheltering ef-  
fects. While the stability had only a small effect on flow dynamics over the flat snow field, it strongly  
influenced the near-surface flow behavior over the concavely shaped snow patch, especially if the  
390 free-stream wind velocity was low. For that experimental setup, the near-surface suppression of  
turbulence was observed to be strongest and the high speed fluid was decoupled from the surface  
enhancing atmospheric stability close to the surface and promoting the cold-air pooling over the  
single snow patch. The atmospheric decoupling was clearly revealed by flux profile measurements  
(strong suppression of momentum and heat fluxes) and by quadrant analysis (strong reduction of ejec-  
395 tions and sweeps in the decoupled region). At higher wind velocities, the strongest turbulent mixing  
was measured much closer to the surface indicating a rush-in of high-momentum fluid of the outer  
layer to the wall region. Below the wind maximum, however, a very shallow layer characterized  
by a suppression of turbulent mixing was still present. Over the flat snow patch, profiles with low  
free-stream wind speeds only involved a weak suppression of the turbulent mixing in a very shal-  
400 low layer above the snow cover. Thus, the strong atmospheric decoupling and cold-air pooling over  
single snow patches appears to be promoted by the cooling effect of the snow in sheltered locations  
causing the local development of a very stable internal boundary layer above the snow patch.

The suppression of heat exchange between the snow surface and the air adjacent to the surface  
effectively slows down snow ablation in spring and promotes the stagnation of the cold air within  
405 topographical depressions covered by snow (Fujita et al., 2010). The process of cold-air pooling  
and atmospheric decoupling is, thus, an important process driving the survival of long-lasting snow  
patches or all-season snow and ice fields in alpine or cold environments. The quantitative contribu-  
tion of the atmospheric decoupling over melting snow for the total mass- and energy balance of a  
complete alpine catchment is not yet known. Although first numerical results of Mott et al. (2015)

410 show that the interaction between boundary layer flow and fractional snow cover significantly affects  
the total energy balance, field measurements conducted over a larger area and for a complete melt  
season are necessary to estimate the relative frequency of phenomena enhancing (advective heat  
transport) or slowing down (atmospheric decoupling) snow melt. Such a comprehensive experimen-  
tal study is currently conducted in a three-years project in an alpine catchment in the Swiss Alps.  
415 Extensive field experiments during the entire ablation period are expected to provide new insight  
into the frequency of described phenomena and the importance for the snow hydrology of the total  
catchment.

*Acknowledgements.* The work presented here is supported by the Swiss National Science foundation SNF  
(Grant:200021\_150146).

## 420 References

- Adrian, R.J., Meinhart, C.D. and Tomkins, C.D.: Vortex organization in the outer region of the turbulent boundary layer. *Journal of Fluid Mechanics*, vol. 422, pp. 1-54, 2000.
- Bodine, D., Klein, P., Arms, S. and Shapiro, A.: Variability of surface air temperature over gently sloped terrain. *J. Appl. Meteorol.* 48, 1117-1141, 2009.
- 425 Burns, P., and Chemel, C.: Evolution of Cold-Air-Pooling Processes in Complex Terrain. *Boundary-Layer Meteorol.* 150, 423-447, doi: 10.1007/s10546-013-9885-z, 2014.
- Collis, D. C., and Williams, M. J.: Two-dimensional convection from heated wires at low Reynolds numbers. *J. Fluid Mech.*, 6, 357-384, doi:10.1017/S0022112059000696, 1959.
- Dadic, R., Mott, R., Lehning, M., and Burlando, P.: Wind Influence on Snow Depth Distribution and Accumulation over Glaciers, *J. Geophys. Res.*, 115, F01012, doi:10.1029/2009JF001261, 2010.
- 430 Daly, C., Conklin, D. R., and Unsworth, M. H.: Local atmospheric decoupling in complex terrain topography alters climate change impacts, *Int. J. Climatol.*, 30, 1857-1864, doi:10.1002/joc.2007, 2010.
- Essery, R.: Modelling fluxes of momentum, sensible heat and latent heat over heterogeneous snowcover, *Q. J. Roy. Meteor. Soc.*, 123, 1867-1883, 1997.
- 435 Essery, R., Granger, R., and Pomeroy, J. W.: Boundary-layer growth and advection of heat over snow and soil patches: modelling and parameterization, *Hydrol. Process.*, 20, 953-967, 2006.
- Fujita, K., Hiyama, K., Iida, H., Ageta, Y.: Self-regulated fluctuations in the ablation of a snow patch over four decades, *Water Resour. Res.*, 46, W11541, doi:10.1029/2009WR008383, 2010.
- Granger, R. J., Pomeroy, J. W., and Essery, R.: Boundary-layer growth and advection of heat over snow and soil patches: field observations, *Hydrol. Process.*, 20, 953-967, 2006.
- 440 Gustavsson, T., Karlsson, M., Bogren, J., Lindqvist, S.: Development of temperature patterns during clear nights, *J Appl Meteorol* 37:559-571, 1998.
- Lehning, M., Löwe, H., Ryser, M., and Raderschall, N.: Inhomogeneous precipitation distribution and snow transport in steep terrain, *Water Resour. Res.*, 44, W09425, doi: 10.1029/2007WR006544, 2008.
- 445 Liston, G. E.: Local advection of momentum, heat and moisture during the melt of patchy snow covers, *Journal of Applied Meteorology*, 34, 1705-1715, 1995.
- Mahrt, L.: Stably stratified atmospheric boundary layers. *Annu. Rev. Fluid Mech.*, 46, 23-45, 2014.
- Mann, J., and Lenschow D. H.: Errors in airborne flux measurements. *J. Geophys. Res.*, 99(D7), 14519-14526, doi:10.1029/94JD00737, 1994.
- 450 Mott, R., Schirmer, M., Bavay, M., Grünewald, T., and Lehning, M.: Understanding snow-transport processes shaping the mountain snow-cover. *The Cryosphere*, 4, 545-559, doi:10.5194/tc-4-545-2010, 2010.
- Mott, R., Egli, L., Grünewald, T., Dawes, N., Manes, C., Bavay, M., and Lehning, M.: Micrometeorological processes driving snow ablation in an Alpine catchment. *The Cryosphere*, 5, 1083-1098, 2011.
- Mott, R., Gromke, C., Grünewald T, and Lehning, M.: Relative importance of advective heat transport and boundary layer decoupling in the melt dynamics of a patchy snow cover, *Advances in Water Resources*, 55, 88-97, doi:10.1016/j.advwatres.2012.03.001, 2013.
- 455 Mott, R., Scipión, D.E., Schneebeli, M., Dawes, N., and Lehning, M.: Orographic effects on snow deposition patterns in mountainous terrain, *J. Geophys. Res. Atmos.*, 119, 1419-1439, doi:10.1002/2013JD019880, 2014.

- 460 Mott, R., Daniels, M., and Lehning, M.: Atmospheric flow development and associated changes in turbulent sensible heat flux over a patchy mountain snow cover, *J. Hydrometeorol.*, 16, 1315-1340, doi: <http://dx.doi.org/10.1175/JHM-D-14-0036.1>, 2015.
- Neumann, N., and Marsh, P.: Local advection of sensible heat in the snowmelt landscape of Arctic tundra, *Hydrol. Process.*, 12, 1547-1560, 1998.
- 465 Ohya, Y.: Wind-Tunnel Study Of Atmospheric Stable Boundary Layers Over A Rough Surface. *Boundary-Layer Meteorology*, 98, 57-82, doi: 10.1023/A:1018767829067, 2001.
- Ohya, Y.: Intermittent bursting of turbulence in a stable boundary layer with low-level jet. *Boundary-Layer Meteorology*, 126, 349-363, doi: 10.1007/s10546-007-9245-y, 2008.
- Price J.D., Vosper S., Brown A., Ross A., Clark P., Davies F., Horlacher V., Claxton B., McGregor J.R., Hoare  
470 J.S., Jemmett-Smith B., and Sheridan P.: COLPEX: field and numerical studies over a region of small hills. *Bull Am Meteorol Soc*, 92,1636-1650, 2011.
- Tabler, R.D.: Predicting profiles of snowdrifts in topographic catchments. In *Western Snow Conference (Colorado, Calif.; April 23-25, 1975)*, Proceedings 43: 87-97, 1975.
- Tropea, C., Yarin, A.L. and Foss, J.F. eds.: *Springer handbook of experimental fluid mechanics*. Springer Science & Business Media, 2007.  
475
- Vosper, S. B., Hughes, J. K., Lock, A. P., Sheridan, P. F., Ross, A. N., Jemmett-Smith, B. and Brown, A. R.: Cold-pool formation in a narrow valley. *Q.J.R. Meteorol. Soc.*, 140: 699-714. doi: 10.1002/qj.2160. 2014.
- Wallace, J.M., Eckelmann, H. and Brodkey, R.S.: The wall region in turbulent shear flow. *Journal of Fluid Mechanics*, 54, 39-48, 1972.
- 480 Whiteman, C.D., Zhong, S., Shaw, W. J., Hubbe, J. M., Bian, X., and Mittelstadt J.: Cold pools in the Columbia basin. *Wea. Forecasting*, 16, 432-447, 2001.
- Whiteman, C.D. and coauthors: METCRAX: Meteorological experiments in Arizonas Meteor Crater. *Bull. Amer. Meteor. Soc.*, 89, 1665-1680, 2008.
- Wilczak, J., Oncley, S., and Stage, S.: Sonic Anemometer Tilt Correction Algorithms, *Bound.-Lay. Meteorol.*,  
485 99, 127-150, doi:10.1023/A:1018966204465, 2001.
- Winstral, A., Elder, K., and Davis, R.E.: Spatial snow modeling of wind-redistributed snow using terrain-based parameters. *J. Hydrometeorol.*, 3, 524-538, 2002.

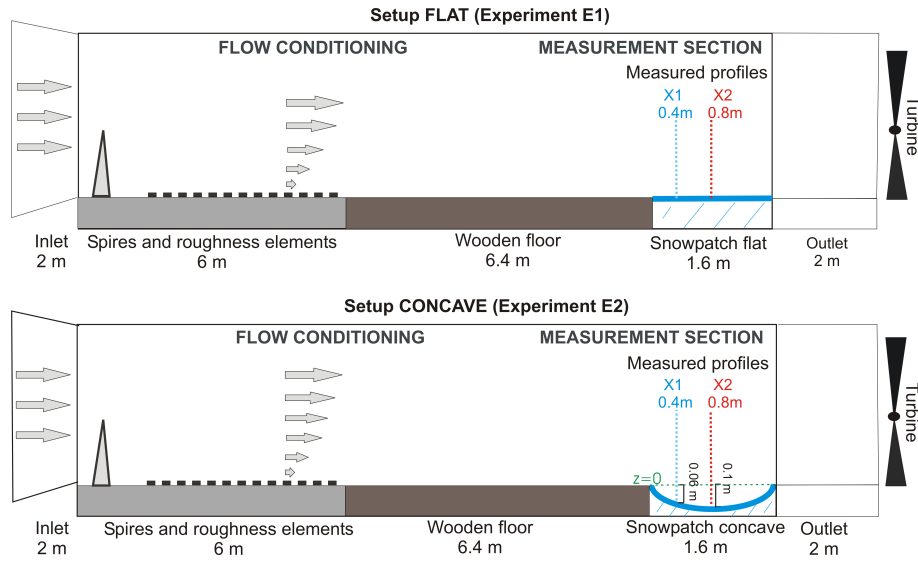


**Figure 1.** Sketch of the SLF boundary layer wind tunnel and measurement setup of experiments 1 (flat setup, E1) and experiment 2 (concave setup, E2). Measurement positions  $X$  are given relative to the leading edge of the snow patch with  $X_0 = -0.1$  m,  $X_1 = 0.4$  m and  $x_2 = 0.8$  m.  ~~$Z_0$  marks the height of the step in topography for the concave setup (E2).~~ Note that all heights  $z$  used in the following figures are relative to the height of the topographical ~~step  $Z_0$ .~~ Consequently for the concave setup, the local surface at  $X_1$  corresponds to  $z = -0.06$  m and at  $X_2$  to  $z = -0.1$  m.

**Table 1.** Experimental setup for six atmospheric profiles with ambient wind velocity  $V_\infty$  ( $ms^{-1}$ ), fetch distance over the snow patch  $X_s$  (m), the bulk Richardson number  $Ri_{bulk}$  and the temperature difference between the surface and the ambient air temperature  $\delta T$  ( $^\circ C$ ). The labels of profiles refer to their position ( $X = X_s$ ), ambient wind velocity ( $U = U_\infty$ ) and the shape of the snow surface (flat = E1; concave = E2).

Profile	$U_\infty$	$X_s$	$Ri_{bulk}$	$\delta T$
E1V1, X1	0.96	+0.4	0.21	8.6
E1V1, X2	0.98	+0.8	0.22	9.2
E1V2, X1	1.94	+0.4	0.05	9.5
E1V2, X2	2.03	+0.8	0.05	9.5
E1V3, X1	3.2	+0.4	0.02	8.6
E1V3, X2	3.33	+0.8	0.02	8.5
E2V1, X1	0.94	+0.4	0.19	12.6
E2V1, X2	0.91	+0.8	0.20	12.5
E2V2, X1	1.93	+0.4	0.04	14.0
E2V2, X2	1.8	+0.8	0.04	13.9
E2V3, X1	2.84	+0.4	0.02	13.0
E2V3, X2	2.84	+0.8	0.02	12.6

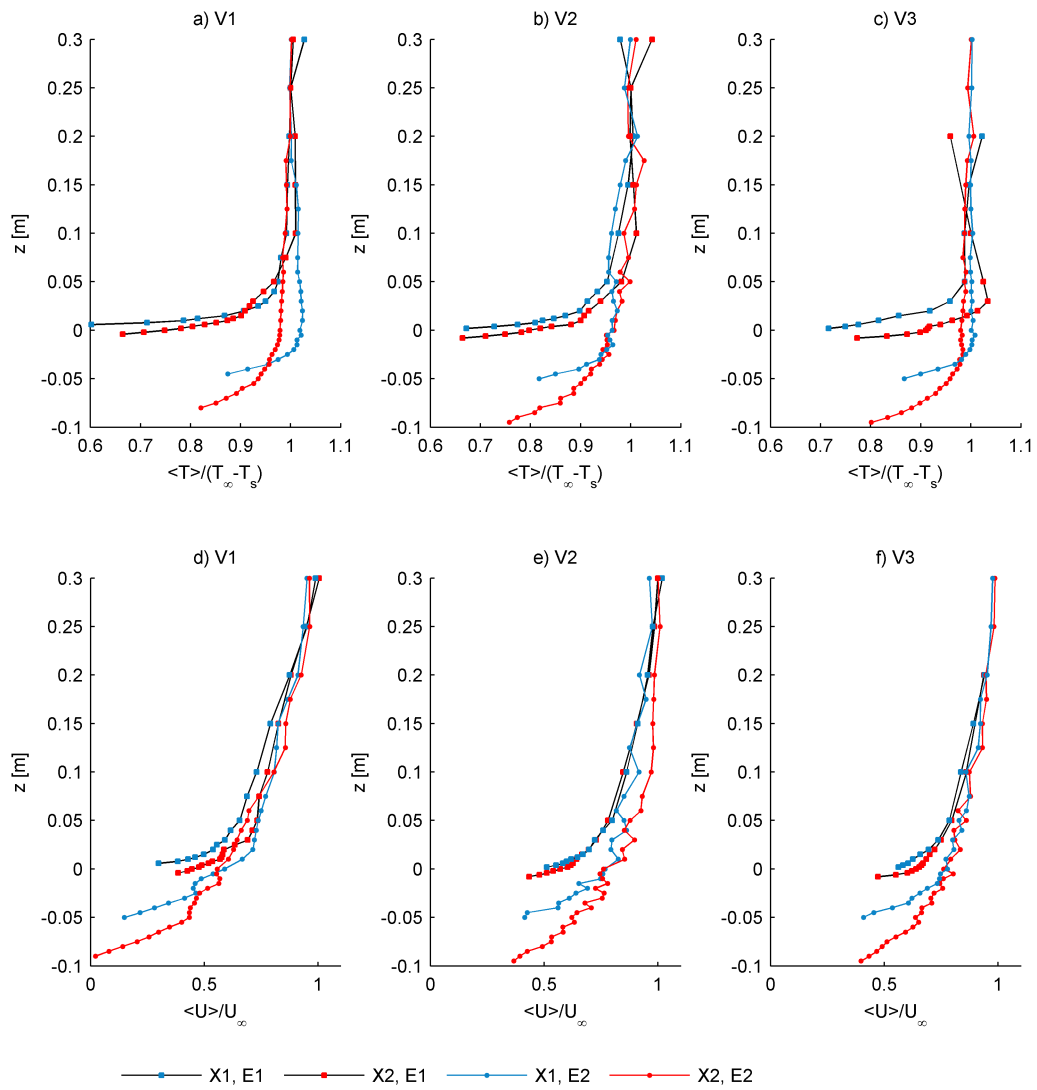


**Figure 2.** Vertical profiles of the mean air temperature (top) and wind velocity (bottom) normalized by the free stream temperature/wind velocity.  $Z_0$  marks the height of the topographical step at  $z=0$  m

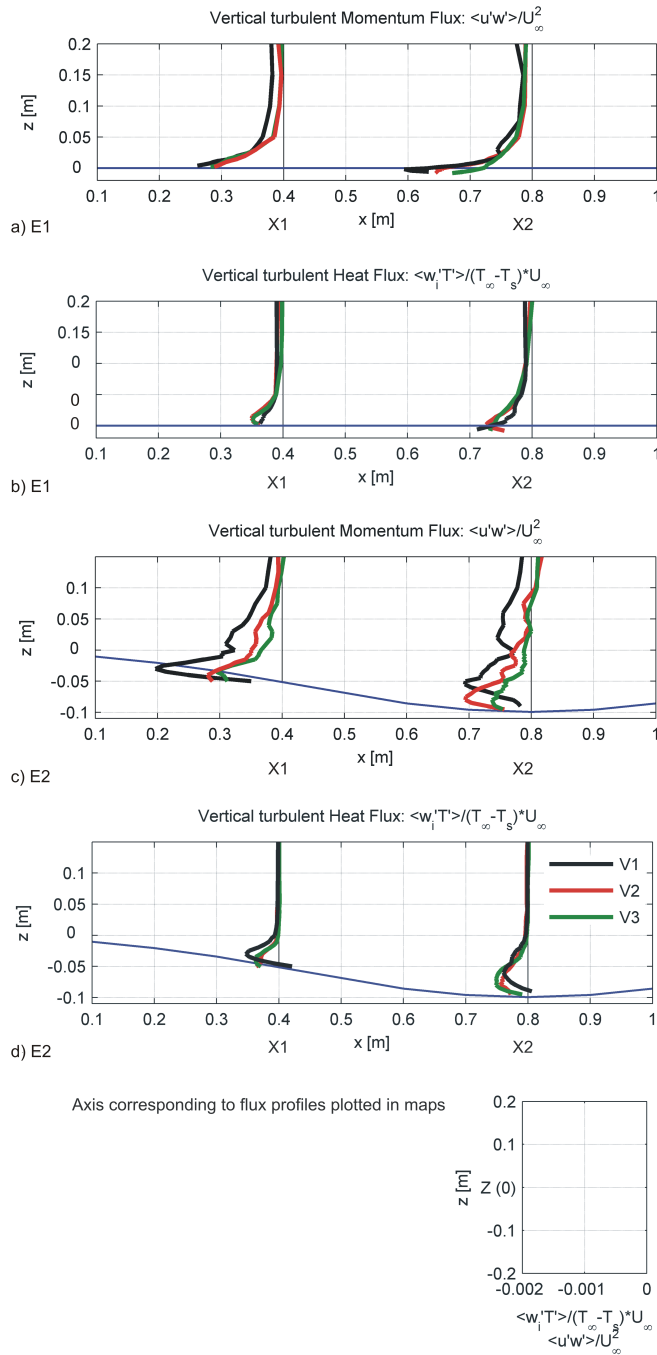


**Figure 3.** Vertical profiles of the turbulent fluxes: momentum flux  $u'w'$  and turbulent vertical heat flux  $w'T'$  normalized by the temperature difference and free stream wind velocity, plotted at the corresponding measurement location along the snow patch for the flat and concave setups. ~~Z0 marks the height of the topographical step at z=0 m.~~ The axis corresponding to the flux profiles is plotted outside of the individual plots.



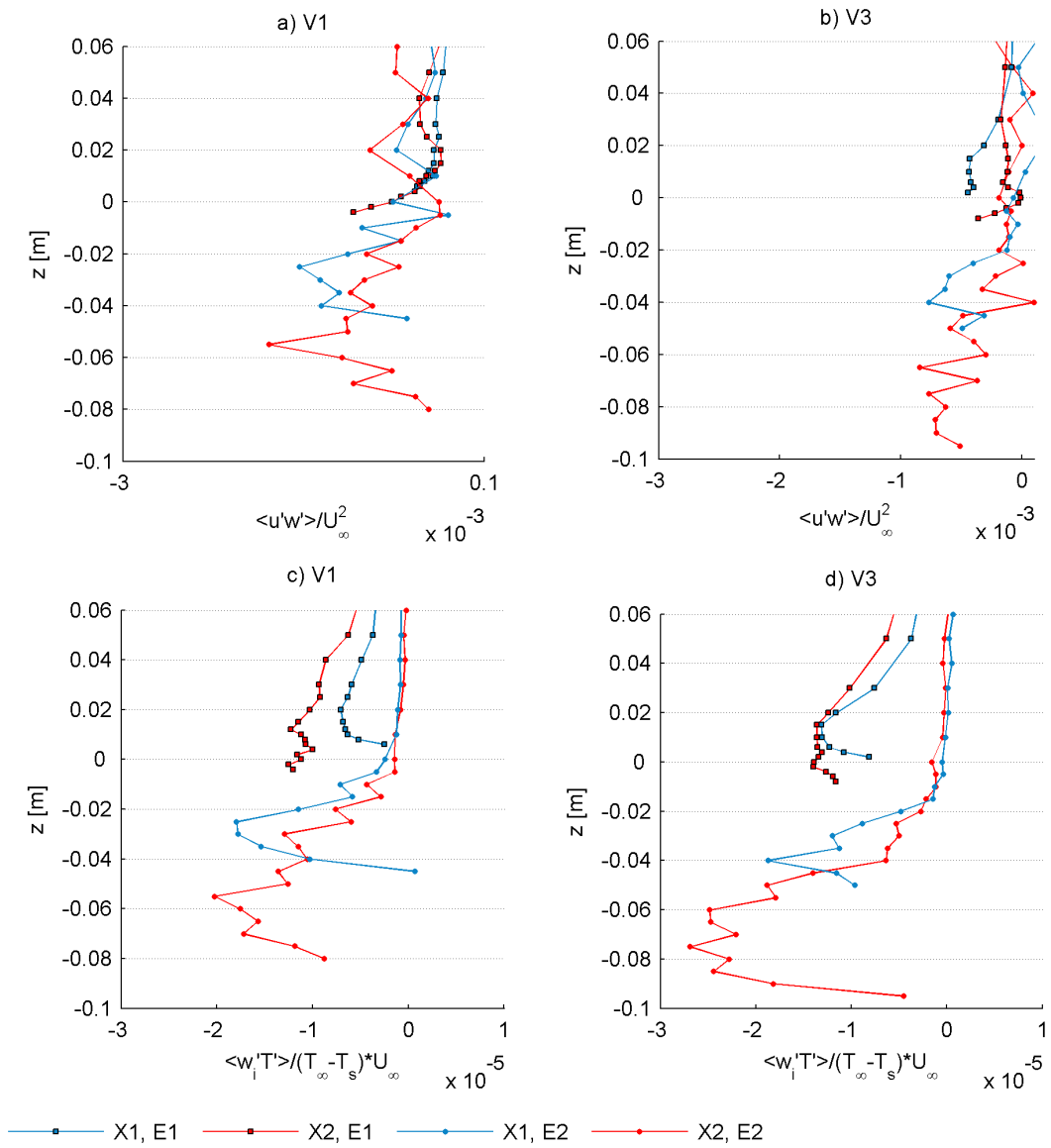


**Figure 4.** Vertical profiles of the turbulent fluxes: momentum flux  $u'w'$  (a, b) and vertical heat flux  $w'T'$  (c, d) normalized by the temperature difference and free stream wind velocity.  $Z_0$  marks the height of the topographical step at  $z=0$  m

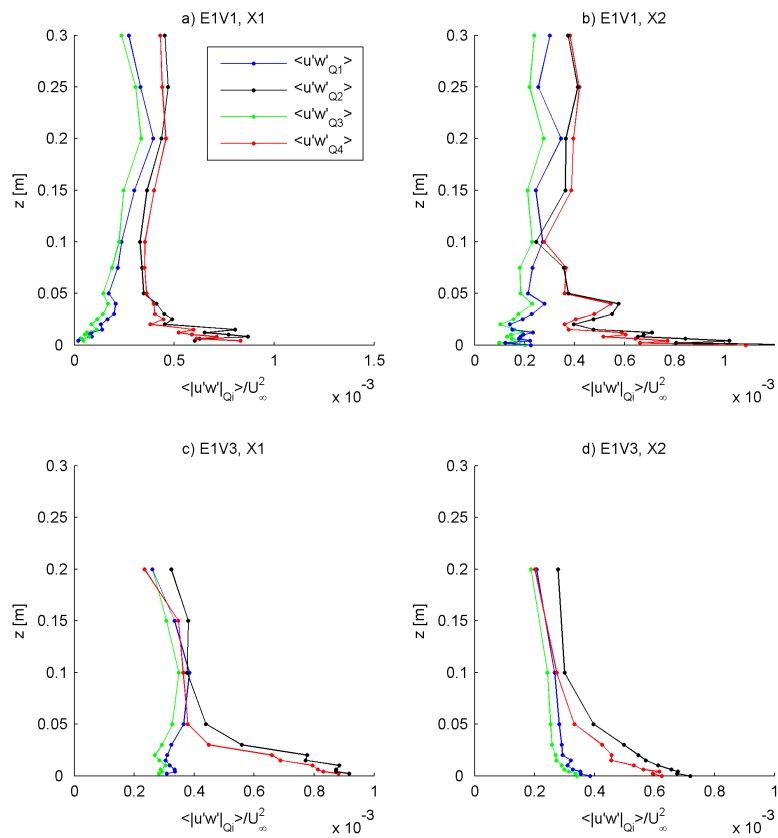


**Figure 5.** Shear stress contribution of the quadrants for the experimental setups E1V1 and E1V3.

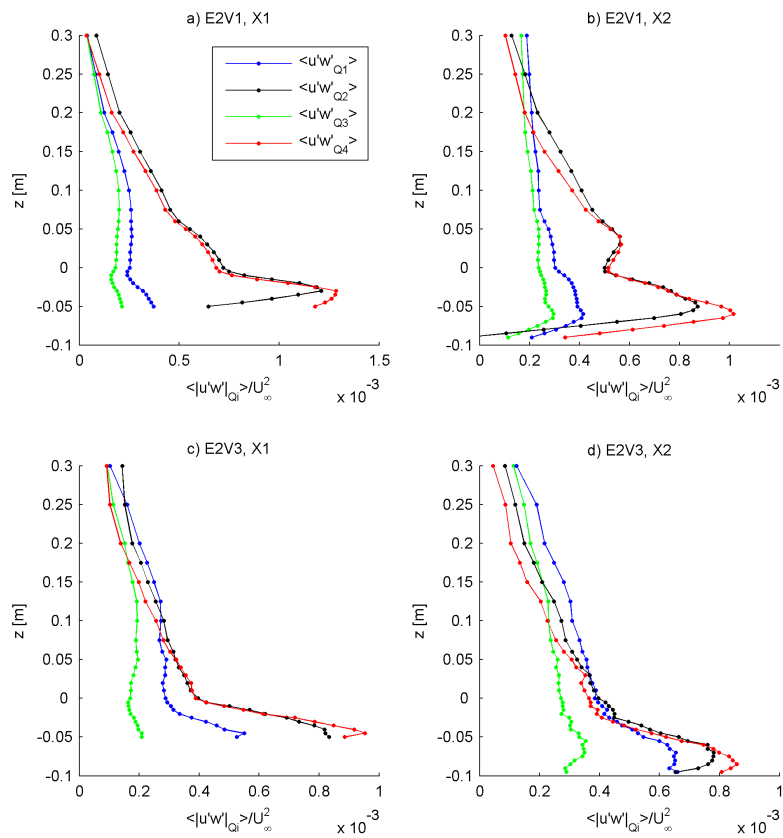


**Figure 6.** Shear stress contribution of the quadrants for the experimental setups E2V1 and E2V3.

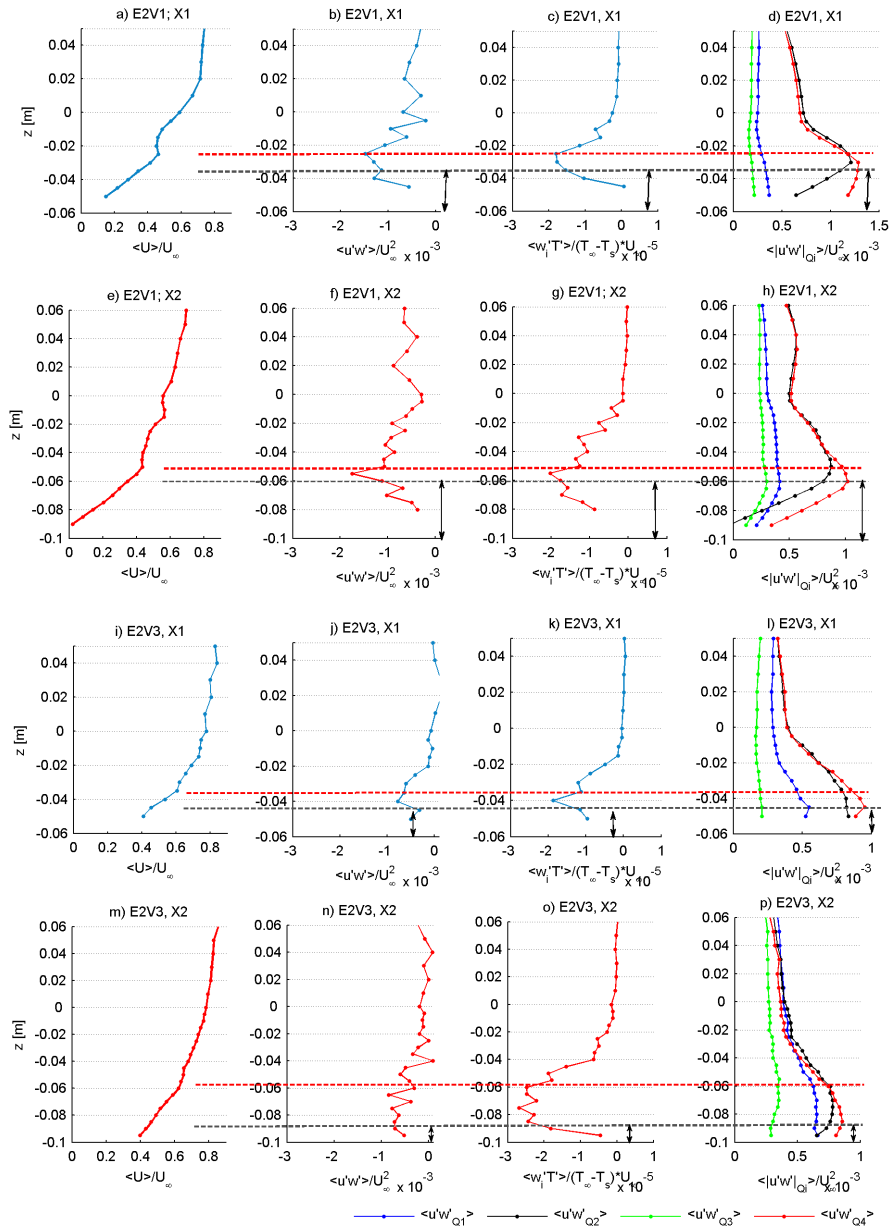


**Figure 7.** Near-surface vertical profiles of mean wind speed, turbulent momentum flux, turbulent heat flux and shear stress distribution over the concave snow patch for experiment E2V1 at measurement location X1 (a-d) and at X2 (e-h) and for experiment E2V3 at X1 (i-l) and at X2 (m-p). ~~Z0 marks the height of the topographical step at z=0 m. Red horizontal lines mark the area of local wind maxima indicating the nose of the low level jet.~~ Horizontal black lines indicate the upper limit of the near-surface suppression of turbulence. The black double-arrow mark the layer, where near-surface turbulence appears to occur.

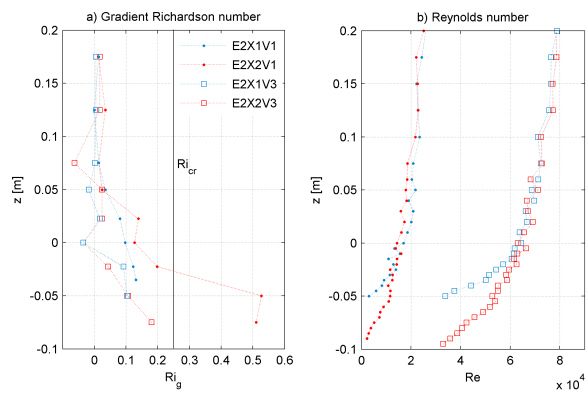


**Figure 8.** Vertical profiles of the a) gradient Richardson number  $Ri_g$  calculated from temperature and wind velocity gradients over a layer of  $dz=0.025$  m and b) Reynoldsnumber  $Re$  calculated from the local wind velocity at each measurement point.